# Spectroscopic Analysis of Stimulated Raman Scattering in the Early Stage of Laser-Induced Breakdown in Water

Hiroharu Yui, Yoshinori Yoneda, Takehiko Kitamori, and Tsuguo Sawada*
*Department of Applied Chemistry, School of Engineering, The University of Tokyo, 7-3-1 Hongo, Bunkyo-ku, Tokyo 113-8656, Japan*
(Received 1 December 1998)

We have investigated laser-induced breakdown (LIB) in water by measuring stimulated Raman scattering (SRS) induced in the early stage of the LIB phenomenon. The SRS is emitted before the breakdown plasma continuum emission becomes dominant and lasts about 80 picoseconds. The time-resolved spectra of the SRS indicate that ice VII structure is formed partially and inhomogeneously in the focal volume of the exciting beam on a picosecond time scale. The mechanism of the SRS inducement is also discussed. [S0031-9007(99)09170-X]

PACS numbers: 78.47.+p, 42.65.–k, 52.50.Jm

Laser-induced breakdown (LIB) refers to plasma production by focusing an intense pulsed laser beam in substances. LIB is a complex phenomenon with various optical, electronic, thermal, and mechanical effects. Considerable effort has been extended for over three decades to understand the LIB phenomenon in various phases [1–16]. In particular, LIB in solids has been extensively studied theoretically and experimentally from several viewpoints, including laser-induced damage of optical materials [5] and applications to x-ray sources [6] and material processing [7], etc. On the other hand, studies of LIB in liquids have concentrated on initial nonlinear optical processes [8–10], shock wave generation [11], cavitation phenomena [12], etc. LIB in water and aqueous solutions is also attracting attention not only in the clarification of fundamental physical process in laser-matter interactions [12,13], but also in applications such as specetrochemical analysis of aqueous media in the environment and industries [14,15] and biomedical utilization in laser surgery [16]. However, the fundamental processes of LIB in liquids are less well understood than that in solids and gases because of their amorphous nature. While experimental and theoretical work has treated the plasma growth in water on a nanosecond or longer time scale [11,12], little is known about the early process of plasma generation and growth on a picosecond time scale. Here we report the observation of stimulated Raman scattering (SRS) induced in the early stage of plasma generation in water. In addition, a structural change in water induced by plasma generation is observed by measuring the time-resolved spectra of the SRS on a picosecond time scale.

A schematic diagram of the experimental setup is shown in Fig. 1. The second harmonic of a Nd-YAG pulse laser (LUMONICS HY200S/MKII; wavelength: 532 nm, pulse duration: 12 ns FWHM and beam diameter: 3 mm) was focused into water in a quartz cell. The spatial profile of the pumping beam was nearly a Gaussian distribution. The focal length of the focusing lens was 100 mm. The maximum optical power density was $4.5 \times 10^{11}$ W cm$^{-2}$ (50 mJ/pulse) in our focusing conditions. This power density is enough to induce breakdown of pure water and some organic solvents [14]. An optical filter (cutoff wavelength 560 nm) was set to reduce the strong background of the pumping beam. An optical fiber was set close to the lateral side of the sample cell to detect plasma emission and Rayleigh scattering of the pumping beam from the same breakdown event. The optical path length from the plasma to the spectrometer (JASCO, CT25CS) was the same for both detection pathways from the forward and lateral sides of the cell. The directivity of the SRS was eliminated by an optical fiber. The focal length of the spectrometer was 250 mm and a grating (150 lines per mm) was set in it. A streak camera system (HAMAMATSUPHOTONICS, U4334-01) was coupled with the spectrometer. A two-dimensional 640 × 480 pixels charge-coupled device (CCD) was set in the streak camera as a detector.

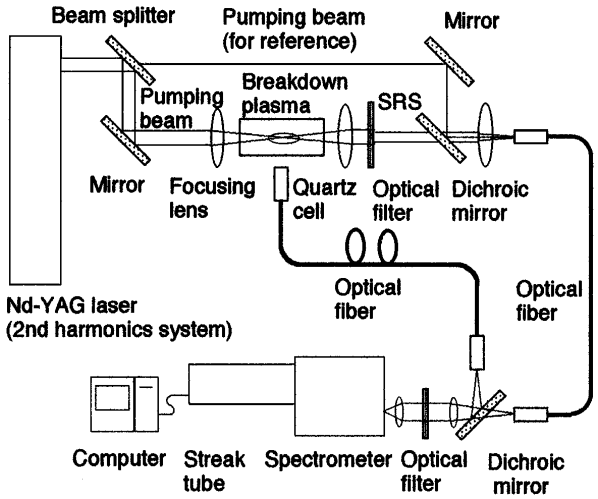


FIG. 1. Schematic diagram of the experimental setup to measure time-resolved spectrum of the SRS, pumping beam, and plasma emission simultaneously.

 0031-9007/99/82(20)/4110(4)$15.00 

The sample was pure water prepared by ultrafiltration (MILLIPORE, Milli-XQ). All experiments were performed at room temperature (293 K).

When we focused the pumping laser pulses, breakdown plasma was generated in water. The SRS of -OH stretching vibrations of water was observed in both forward and backward directions to the pumping beam. Figure 2 shows temporal profiles of the Rayleigh scattering of the pumping beam, plasma continuum emission, and the SRS in the forward direction from the same breakdown event. The optical power density of the pumping beam was $2 \times 10^{11}$ W cm$^{-2}$. The profile of the SRS showed two characteristic features. First, the SRS was emitted before the plasma continuum emission became dominant. Second, the duration of the SRS was about 80 ps for the 12 ns (FHHM) excitation of the pumping beam. These results indicate that the SRS observed here is induced in the very early stage of the plasma generation. It is well known that the -OH stretching vibrations are strongly related to the structure of water. Therefore, the time-resolved spectra of the SRS are expected to provide structural information on water interacting with the growing plasma in the focal volume of the pumping beam on a picosecond time scale.

We measured time-resolved spectra of the SRS. The optical power density of the pumping beam was $2 \times 10^{11}$ W cm$^{-2}$. A spectrum of the SRS is shown in Fig. 3(a). We observed the strongest peak at 3420 cm$^{-1}$, which had shoulders, and a few peaks below 3400 cm$^{-1}$. The Raman shift of the main peak (3420 cm$^{-1}$) corresponded to that of -OH stretching vibrations of water [17]. Of particular interest are the several shoulders and peaks marked by arrows which are not observed in the Raman spectrum of water. Figure 3(b) shows the time courses of these shoulders and peaks with 10 ps resolution. The shoulders and peaks in Fig. 3(a) were grouped into three sets from the differences of their onset times. The first set (● and △) appeared 10 ps after the onset of the SRS emission and the second (●* and △*) and third (●** and △**) sets appeared after 20 and 40 ps, respectively.

The assignment of these peaks was considered as follows. At room temperature, compression of liquid water

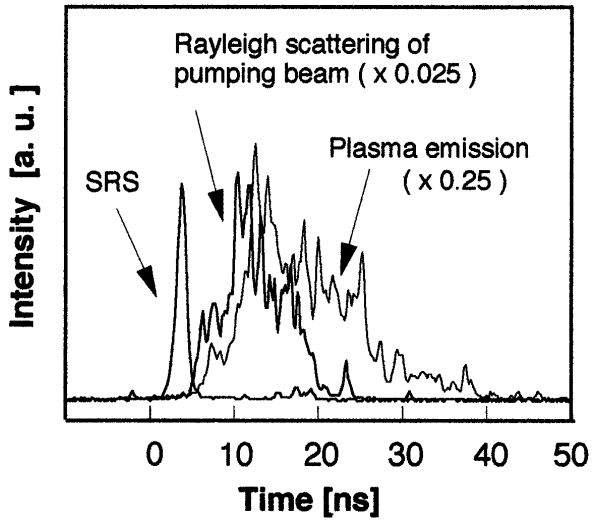


FIG. 2. Temporal profiles of the SRS of water in the forward direction (wavelength range: 645–655 nm), plasma continuum emission (550–600 nm), and Rayleigh scattering of the pumping beam (532 nm) from the same event of laser breakdown. Time resolution was 0.21 ns per CCD pixel.

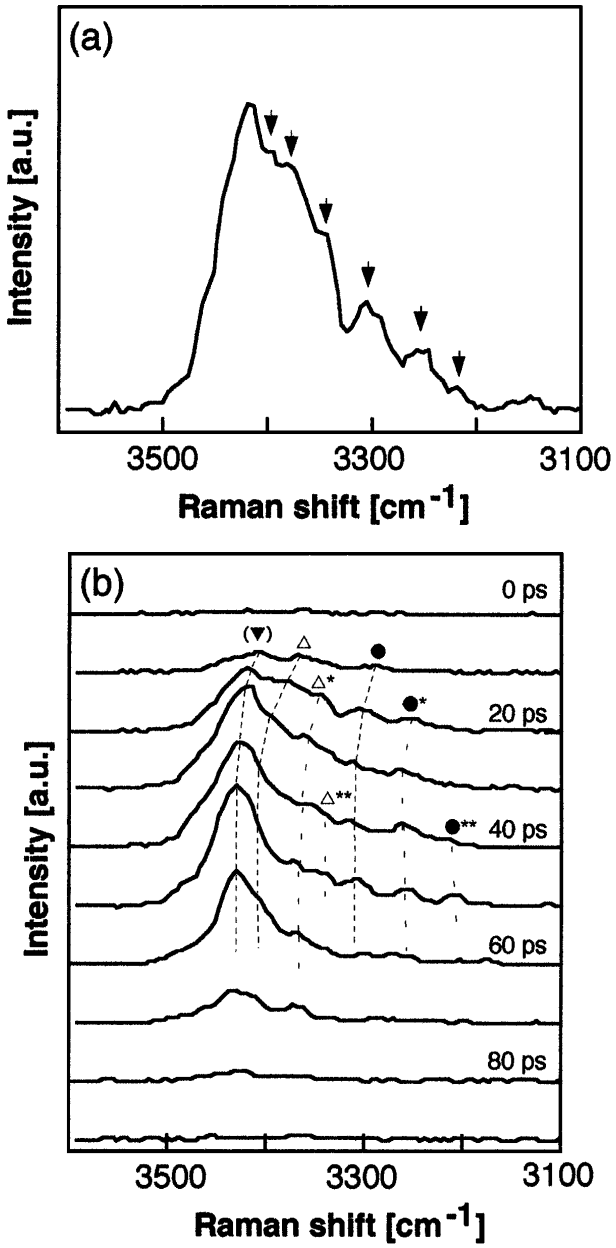


FIG. 3. (a) The spectrum of the SRS. Several shoulders and peaks observed below 3400 cm$^{-1}$ are indicated with arrows. (b) The time-resolved spectra of the SRS. The peak positions of the $A_{1g}$ and $E_g$ modes are indicated as ● and △, respectively. The symbols (●*, △*) and (●**, △**) indicate other sets of peaks of the $A_{1g}$ and $E_g$ modes. The peak position of the $B_{1g}$ mode (▼) is overlapped onto that of the broad and intense -OH stretching mode of water. The time courses of these sets of peaks are indicated as broken lines.

leads to tetragonal ice VI at pressures above 1.05 GPa and further, to cubic ice VII above 2.1 GPa [18]. The Raman peaks of these pressure-induced ice phases appear in the wave number region below 3400 $cm^{-1}$. The Raman shifts of the sets of SRS peaks observed here coincided with those of ice VII [19]. Ice VII gives three characteristic active Raman modes denoted as $A_{1g}, E_g$, and $B_{1g}$. The $A_{1g}$ is the strongest of the three modes and it is assigned to the in-phase symmetric stretching mode. The $E_g$ and $B_{1g}$ modes are assigned to antisymmetric and out-of-phase stretching, respectively. The Raman shifts of the sets of peaks observed here corresponded to those of $A_{1g}$ and $E_g$ modes [19]. It is difficult to identify the $B_{1g}$ mode because it is the weakest of the three modes and its position overlaps the broad and intense SRS peak of water under our experimental conditions. The Raman shifts of the first, second, and third sets of $A_{1g}$ and $E_g$ peaks corresponded to those of ice VII under pressures of about 2.6, 3.6, and 4.5 GPa, respectively. In addition, the first set showed a time-dependent shift which was equivalent to that observed when decreasing pressure from about 2.6 to 2.1 GPa. Although the numbers and Raman shifts of these sets of peaks showed shot-to-shot fluctuations, they corresponded to those of ice VII under 2–5 GPa. These characteristic features of the time-resolved spectra of the SRS indicate that ice VII structure is partially and inhomogeneously formed in the focal volume of the pumping beam on picosecond time scale. Since it is reasonable to assume that the ice VII structure produced by the LIB experiments is of a very local nature, the possibility of the formation of a high density amorphous form of solid water with local structure resembling that of ice VII cannot be ruled out altogether [20]. It is well known that shock waves with GPa pressures are generated in laser-induced plasma production in the liquid medium arising from the confinement effect [12,21]. We consider that the generation of shock waves by plasma production and growth in water is the most probable cause for the formation of ice VII structure.

The optical characteristics of the SRS were measured in order to consider the mechanism of the SRS inducement. Figure 4(a) shows the intensity dependence of the SRS on the optical power density of the pumping beam. Figure 4(b) compares streak images of the SRS under the conditions that the optical power densities of the pumping beam at the beam waist were above and below $4 \times 10^{11}$ W $cm^{-2}$. The intensity of the SRS showed an exponential rise according to the increase of optical power density of the pumping beam when it was below $4 \times 10^{11}$ W $cm^{-2}$ (pumping intensity: 45 mJ/pulse). This intensity dependence is typical of the SRS phenomenon. When the optical power density was about $4 \times 10^{11}$ W $cm^{-2}$ or slightly above, a steep increase of the intensity [Fig. 4(a)], and spectral broadening [Fig. 4(b)] began to be observed. It is well known that when the pumping beam intensity reaches about $10^{12}$ W $cm^{-2}$ or above, self-focusing in water begins to take place [9,22]. The steep increase of the intensity and spectral broadening observed here are typical effects caused by the onset of self-focusing and subsequent self-phase modulation [10]. Therefore, this optical characteristics at $4 \times 10^{11}$ W $cm^{-2}$ can be explained by the onset of these nonlinear optical effects. Above $4 \times 10^{11}$ W $cm^{-2}$, the SRS spectra are rather complicated because these nonlinear optical effects affect the spectral features of the SRS.

In most cases, since the gain for SRS is small for water, enhancement of the effective laser intensity by

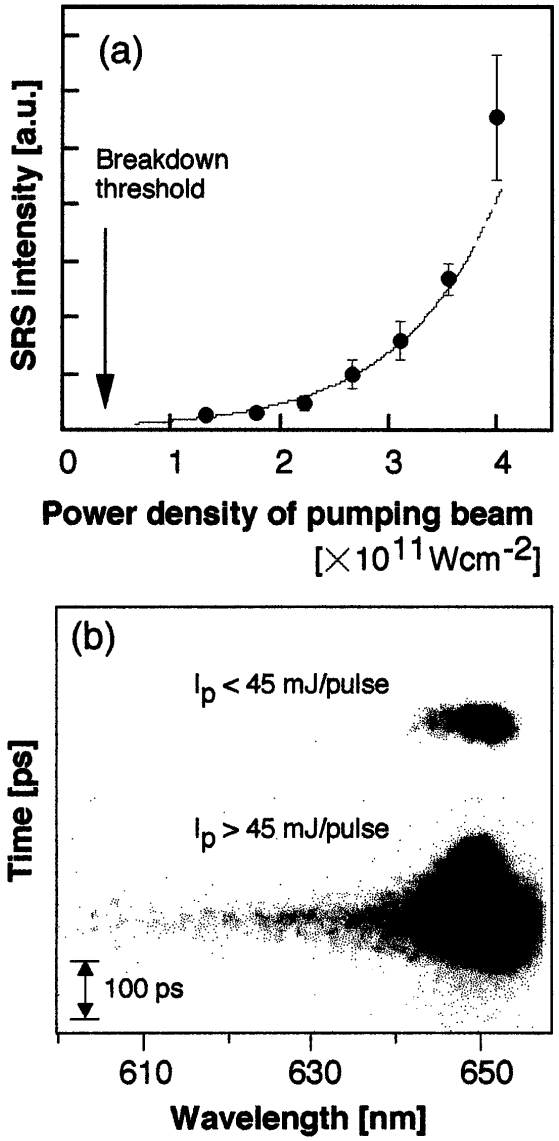


FIG. 4. (a) The dependence of the intensity of the SRS on the optical power density of the pumping beam. The solid line indicates an exponential curve which is fitted to the data when the pumping beam intensity ($I_p$) is below 45 mJ/pulse ($4 \times 10^{11}$ W $cm^{-2}$). (b) Comparison between the streak images of the SRS when the $I_p$ was below (upper image) and above (lower image) 45 mJ/pulse ($4 \times 10^{11}$ W $cm^{-2}$).

self-focusing seems necessary for any appearance of the SRS [9,22]. Thus we should consider other mechanisms dominating the SRS inducement observed below $4 \times 10^{11}$ W cm$^{-2}$. The SRS is a third-order nonlinear process, hence its inducement depends on the third-order nonlinear susceptibility, which is affected mainly by the electronic nonlinear polarizability and the alignment of water molecules. We can assume two factors that contribute to the inducement by plasma generation in water. One is the generation and increase of charged particles such as ions and electrons by plasma production and growth. These charged particles induce a strong electrostatic field ($>$MV cm$^{-1}$) locally and affect the electronic nonlinear polarizability and the alignment of polar molecules. It has been reported that the production of these charged particles induces the nonlinear polarization and drastically changes the nonlinear properties of the medium [22]. The other is the local change of the alignment of water molecules at a charged liquid/plasma interface generated by plasma production in water. The enhancement of nonlinear polarization of water molecules at a charged interface has been reported [23]. To clarify the mechanism of the transient inducement of the SRS, excluding the self-focusing effect, further experiments under much more controlled conditions should be carried out.

In conclusion, we have observed the SRS when laser-induced plasma is generated in water. The SRS was induced in the very early stage of plasma generation and its duration was around 80 ps. The time-resolved spectra of the SRS indicated that the ice VII structure was formed partially and inhomogeneously on a picosecond time scale. The optical characteristics of the SRS showed that the inducement of the SRS could not be explained by well-known nonlinear optical processes such as self-focusing and self-phase modulation. The possibility of the formation of a high density amorphous form of solid water with local structure resembling that of ice VII and the mechanism of the SRS inducement are now under investigation.

G. Wilse Robinson is acknowledged for suggestions that helped improve the paper. This work is supported by Grand-in-Aid for Specially Promoted Research (No.10131218) from the Ministry of Education, Science and Culture of Japan.

*To whom all correspondence should be addressed.

[1] *Laser-Induced Plasma and Applications*, edited by L. Radziemski and D. A. Cremers (Marcel Dekker, New York, 1989).

[2] P. A. Barnes and K. E. Rieckhoff, Appl. Phys. Lett. **13**, 282 (1968).

[3] C. De Michelis, IEEE J. Quantum Electron **5**, 188 (1969).

[4] N. Bloembergen, IEEE J. Quantum Electron. **10**, 375 (1974).

[5] B. C. Stuart *et al.*, Phys. Rev. B **53**, 1749 (1996); Phys. Rev. Lett. **74**, 2248 (1995).

[6] M. D. Perry and G. M. Mourou, Science **264**, 917 (1994); M. M. Murane H. C. Kapteyn, M. D. Rosen, and R. W. Falcone, Science **251**, 531 (1991).

[7] B. P. Fairand and A. H. Clauer, J. Appl. Phys. **50**, 1497 (1979).

[8] R. G. Brewer and K. E. Rieckhoff, Phys. Rev. Lett. **13**, 334 (1964).

[9] A. Penzkofer, A. Laubereau, and W. Kaiser, Phys. Rev. Lett. **31**, 863 (1973).

[10] W. Werncke *et al.*, Opt. Commun. **4**, 413 (1972); W. L. Smith, P. Liu, and N. Bloembergen, Phys. Rev. A **15**, 2396 (1977).

[11] A. Vogel and W. Lauterborn, J. Acoust. Soc. Am. **84**, 719 (1988); H. Schoeffmann, H. Schmidt-Kloiber, and E. Reichel, J. Appl. Phys. **63**, 46 (1988).

[12] S. Siano, R. Pini, R. Salimbeni, and M. Vannini, Appl. Phys. B **62**, 503 (1996).

[13] C. A. Sacchi, J. Opt. Soc. Am. B **8**, 337 (1991).

[14] D. A. Cremers, L. J. Radziemski, and T. R. Loree, Appl. Spectrosc. **38**, 721 (1984).

[15] S. Nakamura, Y. Ito, and K. Sone, Anal. Chem. **68**, 2981 (1996).

[16] P. K. Kennedy, IEEE J. Quantum Electron. **31**, 2241 (1995); **31**, 2250 (1995); J. Gitomer and R. D. Jones, IEEE Trans. Plasma Sci. **19**, 1209 (1991).

[17] See, for example, G. E. Walrafen, J. Chem. Phys. **47**, 114 (1967).

[18] See, for example, H. Shimizu, T. Nabetani, T. Nishiba, and S. Sasaki, Phys. Rev. B **53**, 6107 (1996), and its references.

[19] J. Lin, J. Xu, and E. Huang, J. Geol. Soc. China **38**, 37 (1995); Ph. Pruzan, J. C. Chervin, and M. Gauthier, Europhys. Lett. **13**, 81 (1990); G. E. Walrafen *et al.*, J. Chem. Phys. **77**, 2166 (1982).

[20] G. W. Robinson, S.-B. Zhu, S. Singh, and M. W. Evans, *Water in Biology, Chemistry and Physics: Experimental Overviews and Computational Methodologies* (World Scientific, Singapore, 1996).

[21] C. E. Bell and J. A. Landt, Appl. Phys. Lett. **10**, 46 (1967); P. Teng, N. S. Nishioka, R. R. Anderson, and T. F. Deutsch, IEEE J. Quantum Electron. **23**, 1845 (1987).

[22] H. R. Telle and A. Laubereau, Opt. Commun. **34**, 287 (1980).

[23] X. Zhao and S. Ong, and K. B. Eisenthal, Chem. Phys. Lett. **202**, 513 (1993); D. E. Gragson and G. L. Richmond, J. Phys. Chem. B **102**, 3847 (1998).